JNC TN9400 2001-014

Interpretation of FAENA and TIFFSS experiments : Comparison of temperature evaluation methods on thermal striping

(Research Report)

June 2000

Japan Nuclear Cycle Development Institute
O-arai Engineering Center

KO

JNC TN9400 2001-014
June 2000

Interpretation of FAENA and TIFFSS experiments : Comparison of temperature evaluation methods on thermal striping

(Research Report)

Naoto KASAHARA* and Yves LEJEAIL**

Abstract

Since thermal striping is a coupled thermohydraulic and thermomechanical phenomenon, sodium mock-up tests were usually required to confirm structural integrity. CEA and JNC have developed evaluation procedures of thermal striping to establish design-by-analysis methodology for this phenomenon. In order to compare and to validate these methods, two benchmark problems were planned under EJCC contract. One of benchmarks provided by CEA is temperature and fatigue evaluation of tubes and plates tests performed with the FAENA facility. Another problem from JNC is the same evaluation of plates tests conducted by the TIFFSS facility. This report describes the results of intercomparison of temperature evaluation methods through application to both FAENA and TIFFFSS experiments.

* Structure and Material Research Group, System Engineering Division, OEC, JNC
** CEA-Cadarache DER/SERSI/LECC

JNC TN9400 2001-014
２０００年６月

FAENAおよびTIFFSS試験評価：
サーマルストライピング温度評価法および評価結果の比較

（研究報告書）

笠原 直人*、Yves LEJEAIL**

要　旨

流体温度ゆらぎによる構造物の熱疲労現象は熱流動と構造の両分野に亘る複雑な問題であり、従来その評価にはナトリウムモックアップテストが必要であった。本問題に対する解析による設計法を確立するため、CEAとJNCは評価法の開発を行ってきている。流体温度ゆらぎに対する構造健全性に対して、流体から構造への伝達過程で生じる温度ゆらぎの減衰作用が重要な役割を果たすことが知られている。その減衰の大きさは周波数に依存することから、評価法検証のために周波数制御ナトリウム試験データを用いたベンチマーク問題を計画した。一つはCEAから出題されたもので、温度が周波数制御された平行流を受ける管と平板の温度および疲労評価に関する問題である。もう一つのJNC出題の問題は、周波数制御された垂直ジェットを受ける平板の評価に関するものである。本報告書は両者の実験の温度評価結果について述べる。CEAの流体・構造結合数値計算法およびJNCの周波数応答関数は、温度ゆらぎ減衰の周波数依存性を評価可能であるが、両者とも熱伝達係数の設定が課題であることが分かった。

尚、本内容は1999年9月から2000年8月までの期間にCEAカダラッシュ研究所にて実施した業務の一部である。

*)　大洗工学センター システム技術開発部 構造材料技術開発グループ
**)　CEAカダラッシュ研究所　炉心機器研究室

Contents

List of tables

List of figures

NOMENCLATURE

$T_f(t)$: Temperature of fluid

ΔT_f : Amplitude of sinusoidal temperature fluctuation of fluid

T_{fm} : Average temperature of fluid

$T_s(x,t)$: Temperature of structure

ΔT_s : Amplitude of sinusoidal temperature fluctuation on the structural surface

$T_{s\,max}$: Maximum temperature on the structural surface

$H(t)$: Time response function of effective heat transfer

P, P' : Functions to calculate temperature attenuation and phase delay inside wall

Q, Q' : Functions to calculate temperature attenuation and phase delay inside wall

$\phi\{T_s(x,t)\}$: Thermal stress function determined by mechanical boundary conditions

$H(B_i, jf^*)$: Frequency response function of effective heat transfer

$Bi = \frac{hL}{\lambda}$: Biot number

$t^* = \frac{ta}{L^2}$: Fourier number

$f^* = \frac{fL^2}{a}$: Non-dimensional frequency

μ: $\mu = (\omega / 2a)^{1/2}$

x: Length from the surface of structure

t: Time

f: Frequency of sinusoidal fluctuation

ω: Rotational frequency $\omega = 2\pi f$

h: Heat transfer coefficient

L: Wall thickness of structure

A: Area

R: Moisten length

a: Thermal diffusivity of structural material

λ : Heat conductivity of structural material

c: Specific heat

ρ : Density

q : Heat flux

u : Fluid velocity

u* : Friction velocity

τ : Shear stress in fluid

ν : Kinematic viscosity

α : Thermal diffusivity of fluid

α' : Efective thermal diffusivity of fluid

Pe : Peclet number

Pe* : Turbulent Peclet number

Re : Reynold's number

Pr : Prandtl number

Nu : Nusselt number

y : Distance from the wall toward fluid

1 INTRODUCTION

At an incomplete mixing area of high and low temperature fluids near the structural surface, temperature fluctuation of fluid gives thermal fatigue damage on the wall structures. This coupled thermohydraulic and thermomechanical phenomenon is called thermal striping, which has so complex mechanism and sometimes causes crack initiation on the structural surfaces that sodium mock-up tests are usually required to confirm structural integrity of components.

In order to establish design-by-analysis methodology for thermal striping, CEA and JNC have developed evaluation procedures of this phenomenon. Under EJCC framework, intercomparison of both procedures was planned through application to the common benchmark problems.

One of benchmarks provided by CEA is temperature and fatigue evaluation of tubes and plates due to channel flows [1]. Another problem from JNC is the same evaluation of plates subjected to a vertical jet [1]. The former test was performed by the FAENA facility at CEA-Cadarache. The later one was conducted with the TIFFSS facility at Hitachi Company.

Thermal striping evaluation procedures are divided into temperature analysis methods and fatigue evaluation methods.

The objective of this report is comparison and validation of temperature evaluation methods developed by CEA and JNC through application to FAENA and TIFFSS sodium experiments.

Amplitude of temperature is attenuated during transfer process from fluids to structures. Its attenuation phenomena take an important role on structural integrity and depend on thermal hydraulic conditions in fluids. A fluid condition of FAENA facility is channel flow and inner surfaces of specimens were submitted to fluid temperature fluctuations. Outer surfaces were surrounded by gas environment. On the other hand, TIFFSS facility projects vertical single jet on the inner surfaces of specimens, which were dipped in sodium. It is required in this benchmark problem to evaluate temperature attenuation of both FAENA and TIFFSS experiments.

2. JNC EVALUATION

2.1. FREQUENCY RESPONSE FUNCTION METHOD

2.1.1 EFFECTIVE HEAT TRANSFER FUNCTION

Frequency response function method [4] was utilized to evaluate thermal stress ranges on the structural surfaces induced by fluid temperature fluctuation.

JNC procedure of temperature evaluation based on the frequency response method is summarized here. The first step is identification of the following parameters from frequency of temperature fluctuation, heat transfer coefficient and material properties of structures.

Non-dimensional frequency :

$$f^* = \frac{fL^2}{a} \tag{2.1}$$

Biot number :

$$Bi = \frac{hL}{\lambda} \tag{2.2}$$

The second step is determination of the effective heat transfer function,

$$H = \mathrm{H}(B_i, jf^*) \tag{2.3}$$

from above two parameters. Both formula and the following diagram provide gains of effective heat transfer function as a function of non-dimensional frequency and Biot number.

$$\left|\mathrm{H}(B_i, jf^*)\right| = \frac{B_i}{\sqrt{\left(B_i + \sqrt{\pi f^*}\right)^2 + \pi f^*}} \tag{2.4}$$

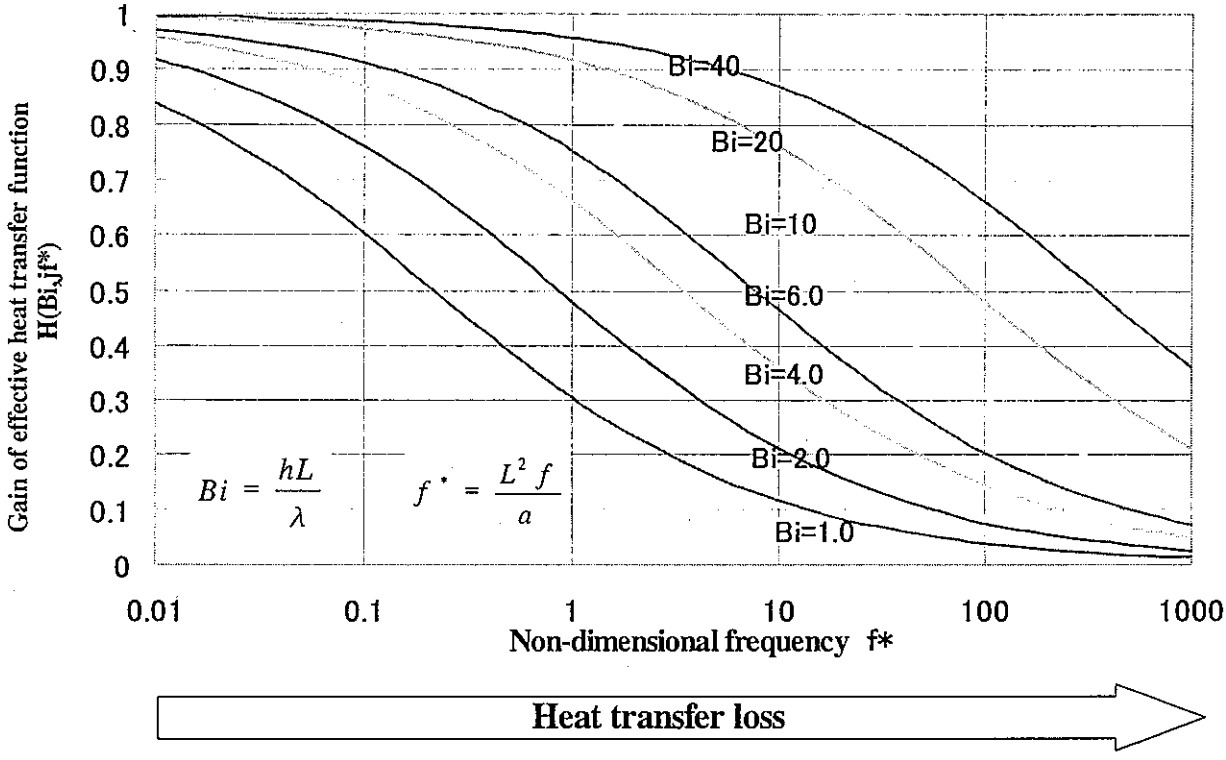

Fig.2.1 Gain of effective heat transfer function

By using effective heat transfer function, the temperature amplitude and the maximum temperature on the structural surface were determined from fluid temperature as

$$\Delta T_s = |H| \Delta T_f \tag{2.5}$$

$$T_{s\max} = T_{fm} + \frac{1}{2}|H|\Delta T_f \tag{2.6}$$

2.1.2 EXPERIMENTAL GAINS OF FAENA AND TIFFSS

Average of fluid temperature of the FAENA 4th experiment is 400℃. By using material properties of 316L(N) at 400 ℃ [1] and wall thickness 15mm, non-dimensional frequencies were evaluated from actual ones. Non-dimensional frequencies of TIFFSS-3 experiment were calculated by the same way with average fluid temperature 350 ℃ and wall thickness 10mm,.

Here let us introduce experimental gains of heat transfer from fluids to structures $|H|^{exp}$ defined between measured temperature amplitudes on the structural surface $\Delta T_s{}^{exp}(0)$ and fluid temperature amplitude at distance d from the structural surface $\Delta T_f{}^{exp}(d)$ as

$$|H|^{exp} = \frac{\Delta T_s{}^{exp}(0)}{\Delta T_f{}^{exp}(d)}. \tag{2.7}$$

FAENA 4th series measured fluid temperature at points of 2mm and 5mm distances from the surface[2]. In TIFFSS-3 series, measurement points of fluid temperature were at distances of 0.5mm, 1.5mm, and 5.5mm (outlet of the nozzle) distance from the surface. Experimental gains of heat transfer $|H|^{exp}$ were calculated for each of above distances.

Relations between $|H|^{exp}$ and f^* were evaluated for each fluid measurement point of FAENA 4th series and TIFFSS-3 as shown in Table 2.1 , Table 2.2 and Fig.2.2.

Table 2.1(a) Experimental gain of heat transfer of FAENA 4th

f (Hz)	f*	FAENA-4th (L=15mm,d=5mm)
0.05	2.49	0.82
0.07	3.48	0.79
0.10	4.98	0.75
0.13	6.22	0.73
0.17	8.26	0.67
0.25	12.44	0.55

Table 2.1(b) Experimental gain of heat transfer of FAENA 4th

f (Hz)	f*	FAENA-4th (L=15mm,d=2mm)
0.05	2.49	0.94
0.07	3.48	0.94
0.10	4.98	0.91
0.13	6.22	0.89
0.17	8.26	0.87
0.25	12.44	0.84

Table 2.2(a) Experimental gain of heat transfer of TIFFSS-3

f (Hz)	f*	Tiffss-3 (L=10mm,d=5.5mm)
0.01	0.23	0.85
0.02	0.45	0.84
0.04	0.91	0.81
0.10	2.26	0.72
0.20	4.53	0.64

Table 2.2(b) Experimental gain of heat transfer of TIFFSS-3

f (Hz)	f*	Tiffss-3 (L=10mm,d=1.5mm)
0.01	0.23	0.99
0.02	0.45	0.98
0.04	0.91	0.98
0.10	2.26	0.96
0.20	4.53	0.94

Table 2.2(c) Experimental gain of heat transfer of TIFFSS-3

f (Hz)	f*	Tiffss-3 (L=10mm,d=0.1mm)
0.01	0.23	0.98
0.02	0.45	0.98
0.04	0.91	0.98
0.10	2.26	0.96
0.20	4.53	0.95

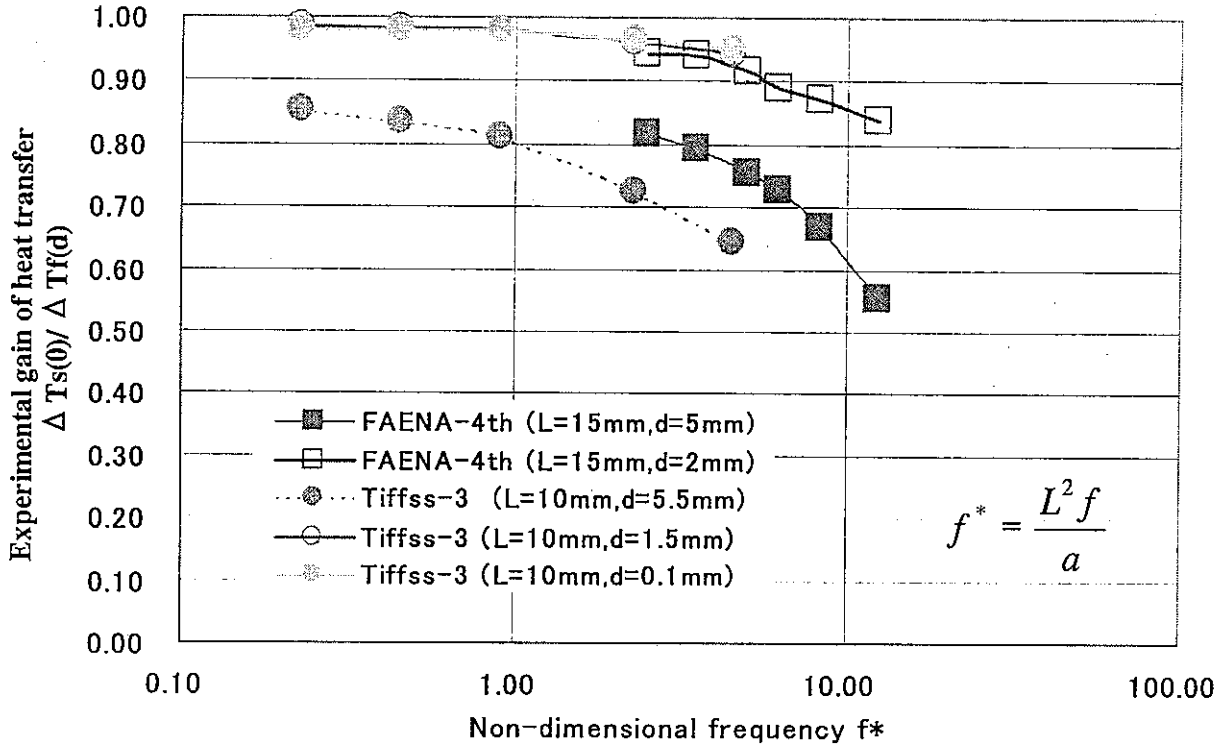

Fig.2.2 Experimental gain of heat transfer of FAENA 4th and TIFFSS-3

It is understood from Fig.2.2 that gain of heat transfer decreases when frequency or distance between fluid and structural surface increases.

These characteristics agree with tendency of the effective heat transfer function.

2.1.3 HEAT TRANSFER COEFFICIENT

The effective heat transfer function requires heat transfer coefficients and their conversion to Biot numbers.

One of methods to obtain heat transfer coefficients is utilization of heat transfer equations.

There are several options of heat transfer equations for the channel flow of FAENA 4th. Among them, Skupinski equation[3] for turbulent convection in tubes

$$Nu = 4.82 + 0.0185 Pe^{0.827} \tag{2.8}$$

is usually adopted in CEA.

In the case of square sections, equivalent diameter D_H can be calculated by

$$D_H = \frac{4A}{R}. \tag{2.9}$$

On the other hand, JNC typically uses Subbotine (Seban-Shimazaki) equation

$$Nu = 5 + 0.025 Pe^{0.8}. \tag{2.10}$$

For considering scatter of heat transfer coefficients, 2 kinds of heat transfer equations were utilized to determine Biot numbers as in the next table.

Table 2.3 Heat transfer coefficient and Biot number of FAENA 4th

Skupinski	h=20200kcal/m^{2}h/°C Bi=18.2
Subbotin	h=21500kcal/m^{2}h/°C Bi=19.3

TIFFSS-3 is a single vertical jet and there are some difficulties to apply heat transfer equations, because a vertical jet is composed of potential core and progress regions and its heat transfer coefficient changes according to distance from the nozzle. Distance from the nozzle of TIFFSS-3 is considered as a potential core region and *Gardon's* equation

$$Nu = 0.535\,\mathrm{Pr}^{0.4}\,\mathrm{Re}^{0.5}. \tag{2.11}$$

is suitable. Eq.(2.11) estimated heat transfer coefficient of TIFFSS-3 as 76400kcal/m2h℃.

In the case of the TIFFSS-4 plate specimen with insulator, temperature distribution across wall thickness was measured under steady state (0Hz frequency). Since TIFFSS-3 plane specimen is almost the same as the TIFFSS-4, these data can be utilized to estimate heat transfer coefficient for TIFFSS-3 specimen. The following graph shows measured temperature distribution across wall thickness under both steady states of high temperature injection and low temperature one. A linear interpolation method converted measured temperatures to temperature gradient dT/dx in direction of wall thickness as shown in the next graph.

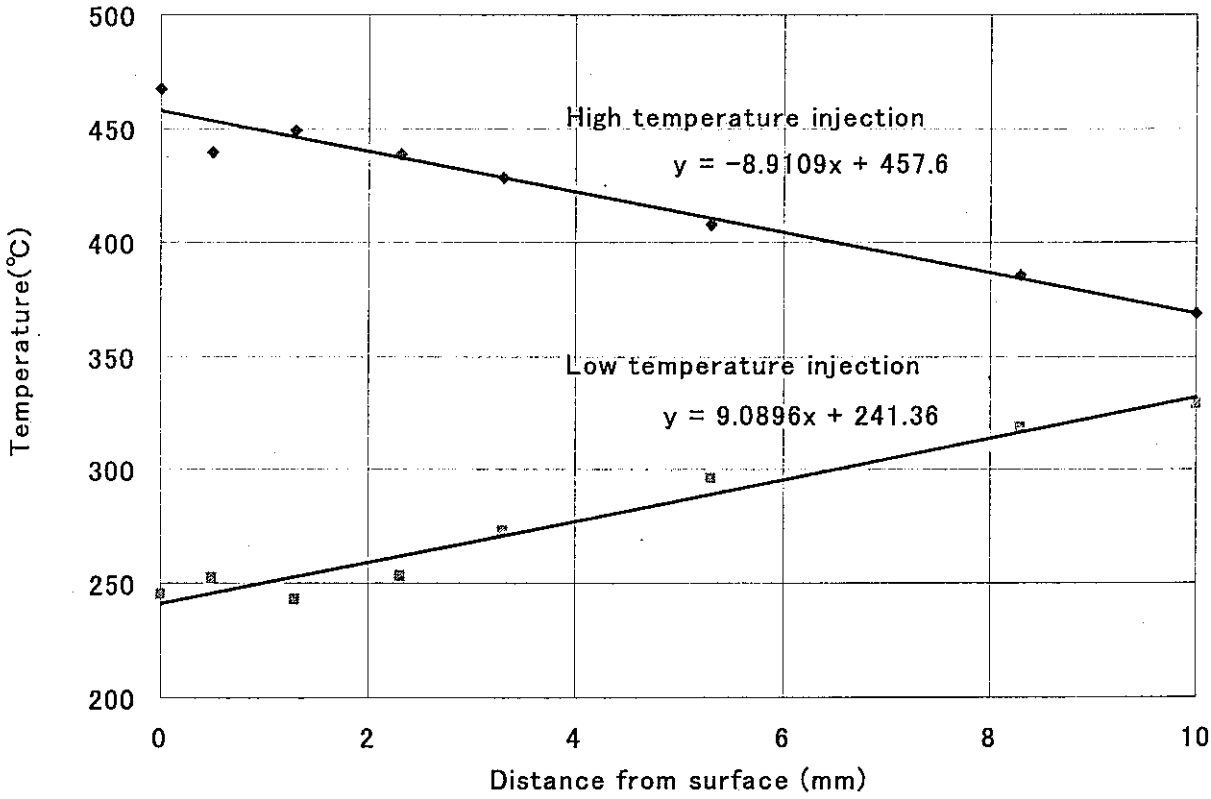

Fig.2.3 Measured temperature gradients and these interoperations of TIFFSS-4

Heat conductivity of materials can interpret temperature gradients to heat fluxes as

$$q = \lambda \frac{dT}{dx}. \tag{2.12}$$

Heat transfer coefficients were evaluated from heat fluxes and temperature differences between structural surfaces T_s and fluid $T_f(d)$ measured at distances d from surfaces as

$$q = h\left(T_f(d) - T_s\right). \tag{2.13}$$

The next table shows the evaluated heat transfer coefficients.

Table 2.4 Heat transfer coefficient evaluated from TIFFSS-4 experiment

	T/d (°C/mm)	λ (kcal/mmsec°C) at average temperature	q(kcal/mm^{2}sec)	H(kcal/m^{2}h°C) d=5.5	H(kcal/m^{2}h°C) d=1.5	H(kcal/m^{2}h°C) d=0.5
High temperature injection	8.91	4.73	42.2	1.27E+04	2.42E+04	2.02E+05
Low temperature injection	9.09	4.34	39.4	1.39E+04	2.17E+04	5.26E+04
Average			40.8	1.33E+04	2.30E+04	1.27E+05

Biot numbers corresponding to above heat transfer coefficients are summarized in the next table.

Table 2.5 Heat transfer coefficient and Biot number for TIFFSS-3

	H(kcal/m^{2}h°C)	Bi
Gardon	76400	46.9
TIFFSS-4 Exp. (d=5.5mm)	13300	8.19
TIFFSS-4 Exp. (d=1.5mm)	23000	14.1
TIFFSS-4 Exp. (d=0.5mm)	127000	78.2

2.1.4 EVALUATION OF GAINS OF HEAT TRANSFER

By using Biot number in Table 2.3, the effective heat transfer function defined by Eq.(2.4) calculated gains of FAENA 4th and they were compared with experimental ones as in the next figure and the table.

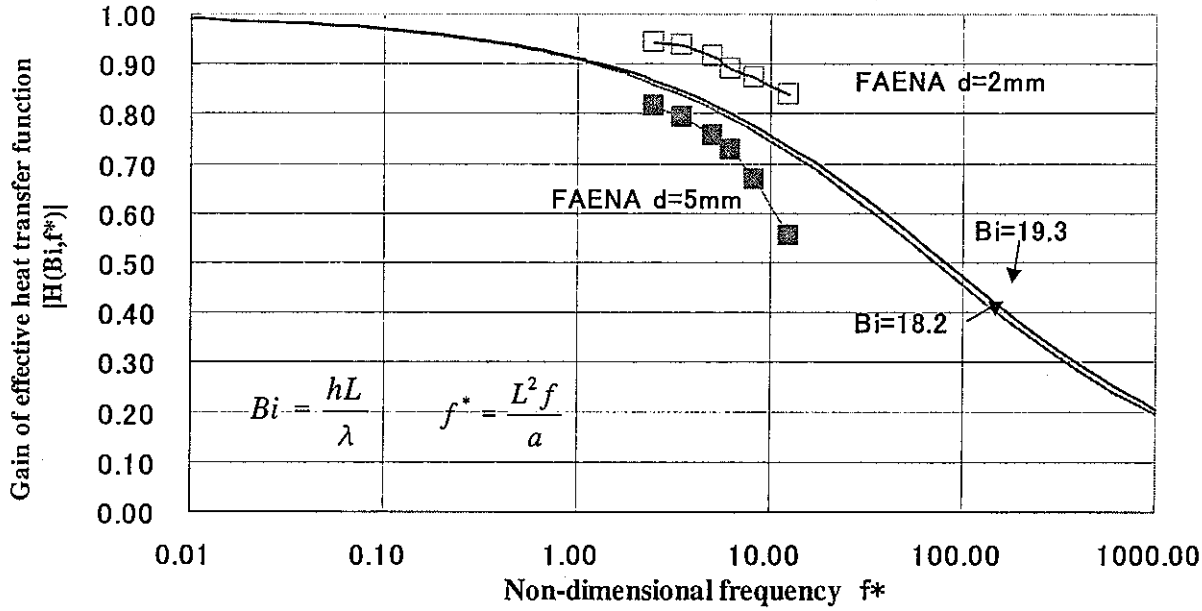

Fig.2.4 Measured and predicted gains of heat transfer of FAENA 4th

Table 2.6 Measured and predicted gains of heat transfer of FAENA 4th

f (Hz)	Non-dimensional frequency f*	Biot number	FAENA-4th (L=15mm,d=5mm) Measured gains	FAENA-4th (L=15mm,d=5mm) JNC Predicted gains
0.05	2.49	19.3	0.82	0.87
0.07	3.48	19.3	0.79	0.84
0.10	4.98	19.3	0.75	0.82
0.13	6.22	19.3	0.73	0.80
0.17	8.26	19.3	0.67	0.77
0.25	12.44	19.3	0.55	0.73

In Fig.2.4, deviation of gains from scatter of Biot numbers is small and predicted gains are closer to measurement at 5mm than one at 2mm. There is a possibility that fluid at distance of 2mm is affected from a boundary layer in spite that heat transfer coefficients evaluated from above equations are defined for main flow.

By using Biot number in Table 2.5, the effective heat transfer function evaluated gains of TIFFSS-3 and were compared with experimental data as in the next figure and the table.

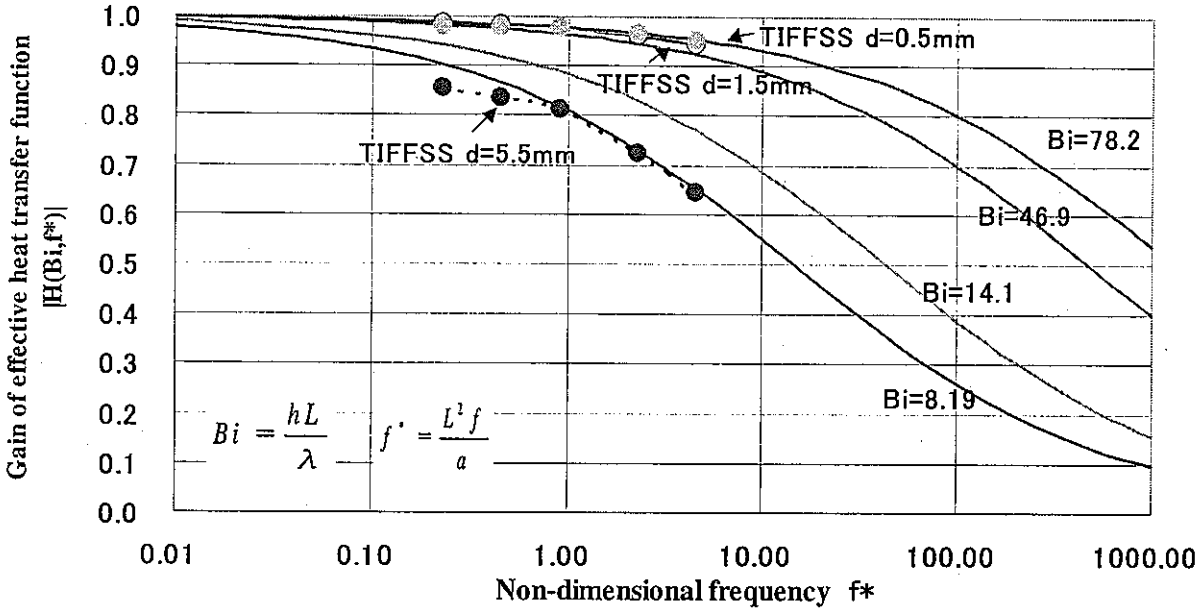

Fig.2.5 Measured and predicted gains of heat transfer of TIFFSS-3

Table 2.7 Measured and predicted gains of heat transfer of TIFFSS-3

f (Hz)	Non-dimensional frequency f*	Biot number	Tiffss-3 (L=10mm,d=5.5mm) Measured gains	Tiffss-3 (L=10mm,d=5.5mm) JNC Predicted gains
0.01	0.23	8.19	0.85	0.90
0.02	0.45	8.19	0.84	0.87
0.04	0.91	8.19	0.81	0.82
0.10	2.26	8.19	0.72	0.73
0.20	4.53	8.19	0.64	0.65

Predicted gains with experimental heat transfer coefficients at 5.5mm and 0.5mm have good correlation with measured ones at distance of 5.5mm and 0.5mm. However, predictions by *Gardon's* equation are far from all experimental results and evaluated results by the experimental coefficient at 1.5mm have large differences from experimental gains. The *Gardon's* equation of Eq.(2.11) is independent from distance between fluid and structures within 24mm of distance, since this region is considered within potential core where temperature is homogeneous. Here a diameter of potential core is usually smaller than an inner diameter of a nozzle. On the other hand, all thermocouples except at a nozzle locate outside of the diameter of nozzle. Therefore actual measurement points are outside of the potential core. It is why the *Gardon's* equation was not appropriate for TIFFSS-3.

The next figure compares the FAENA and TIFFSS experimental data and effective heat transfer functions with various Biot numbers. This figure shows that there exists constant heat transfer coefficient that is independent from frequency of temperature fluctuation. So that rational evaluation methods of effective heat transfer coefficient are desired.

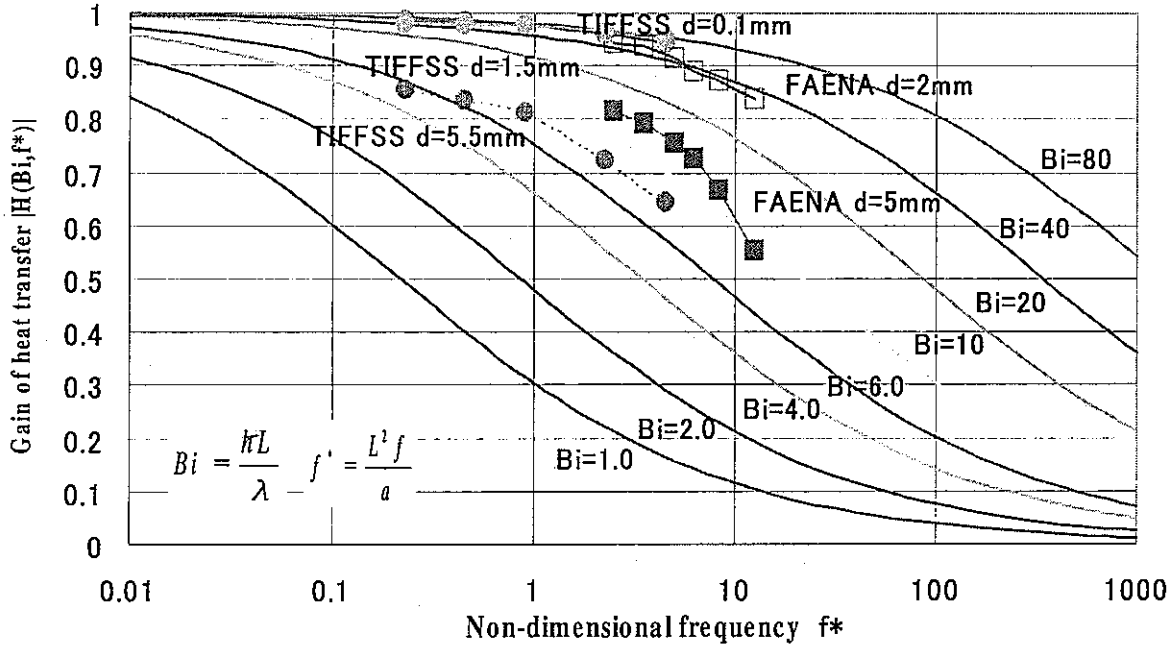

Fig.2.6 Measured gains of heat transfer and effective heat transfer function

2.2. FINITE ELEMENT METHOD

One of the objectives of Finite element calculations is to evaluate influences of thermal boundaries from back surfaces. This study will validate adequacy of a semi-infinite solid model of the Frequency response function method. Another purpose is to study difference between sinusoidal temperature fluctuation and actual temperature one in experiments. The last objective is to investigate sensitivity of thermal stress to temperature dependency of material properties.

(1) Influences of thermal boundaries of back surfaces

Since TIFFSS experiments have thinner specimens than FAENA ones and back side of specimen was attached to sodium(350℃), thermal boundaries from back surfaces have larger influences on thermal stresses on the surface. So that, influences of thermal boundaries from back surfaces were investigated with a temperature calculation model of TIFFSS-3 shown in Fig.2.7. Heat transfer coefficient on the surface was assumed to be 12000kcal/m^2℃, which corresponds to Bi=7.36. For the back surface, both adiabatic condition and 2000kcal/m^2℃ heat transfer condition were hypothesized. In order to get stable solutions, 10 cycles of fluctuations were calculated. FINAS code[8] performed finite element calculations with a mesh model with isoparametric plane elements(Fig.2.8). Temperature dependency of material properties was considered.

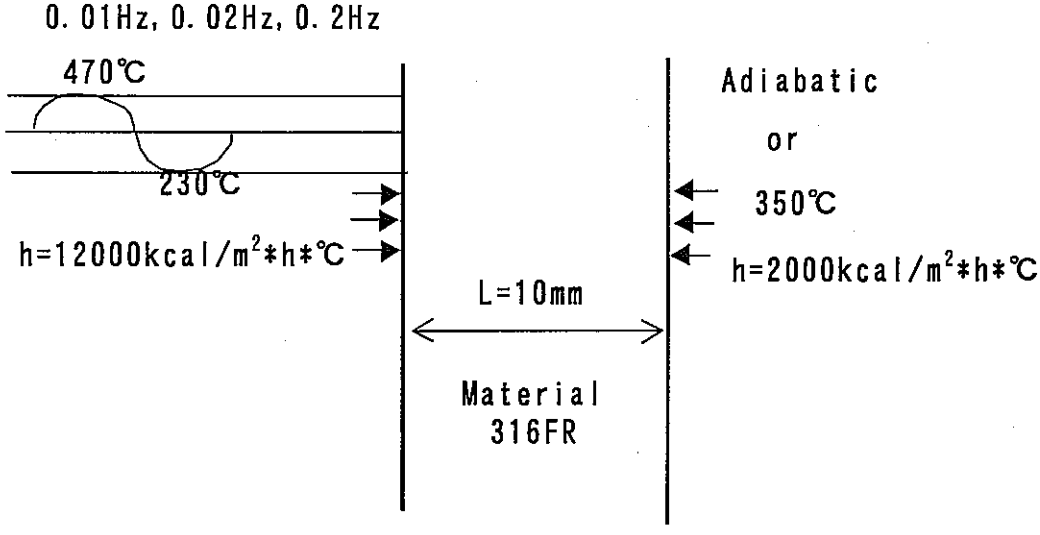

Fig.2.7 Temperature calculation model with boundary condition for TIFFSS-3

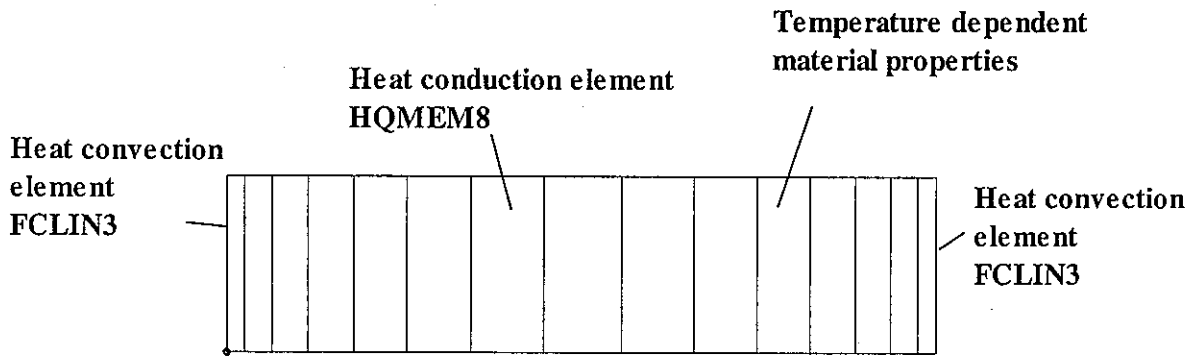

Fig.2.8 Finite element model for TIFFSS-3

Fig. 2.9 shows temperature distributions when the temperature on the inner surface is the maximum and the minimum. Fig. 2.10 exhibits distributions of the maximum and the minimum temperature, at each point during temperature fluctuation. These figures explain that temperature amplitude on the inner surface is insensitive to boundary conditions of back surface, even though temperature amplitudes on the back surface are very different.

Fig.2.11 compares gains of temperature amplitude from fluids to structures among experimental results, predictions by frequency response method and F.E. calculations. These results clarified that influence from backside is negligible and a semi-infinite model is adequate.

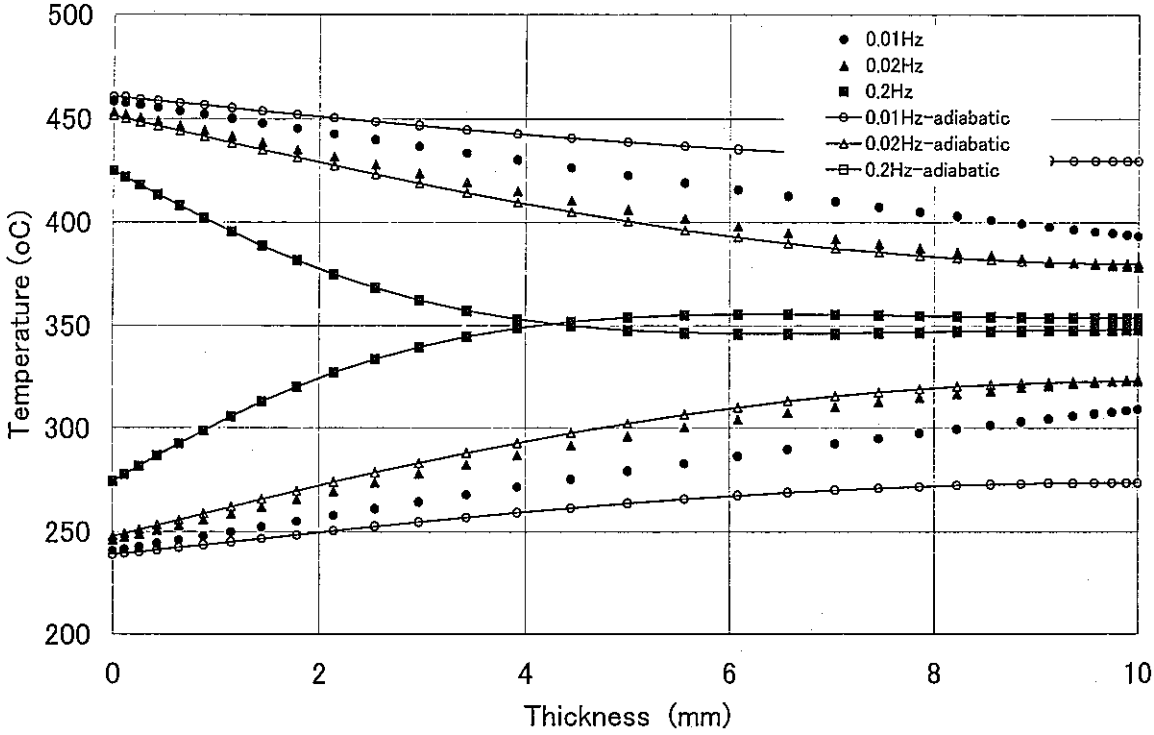

Fig. 2.9 Temperature distribution when the temperature on the inner surface is the maximum and the minimum

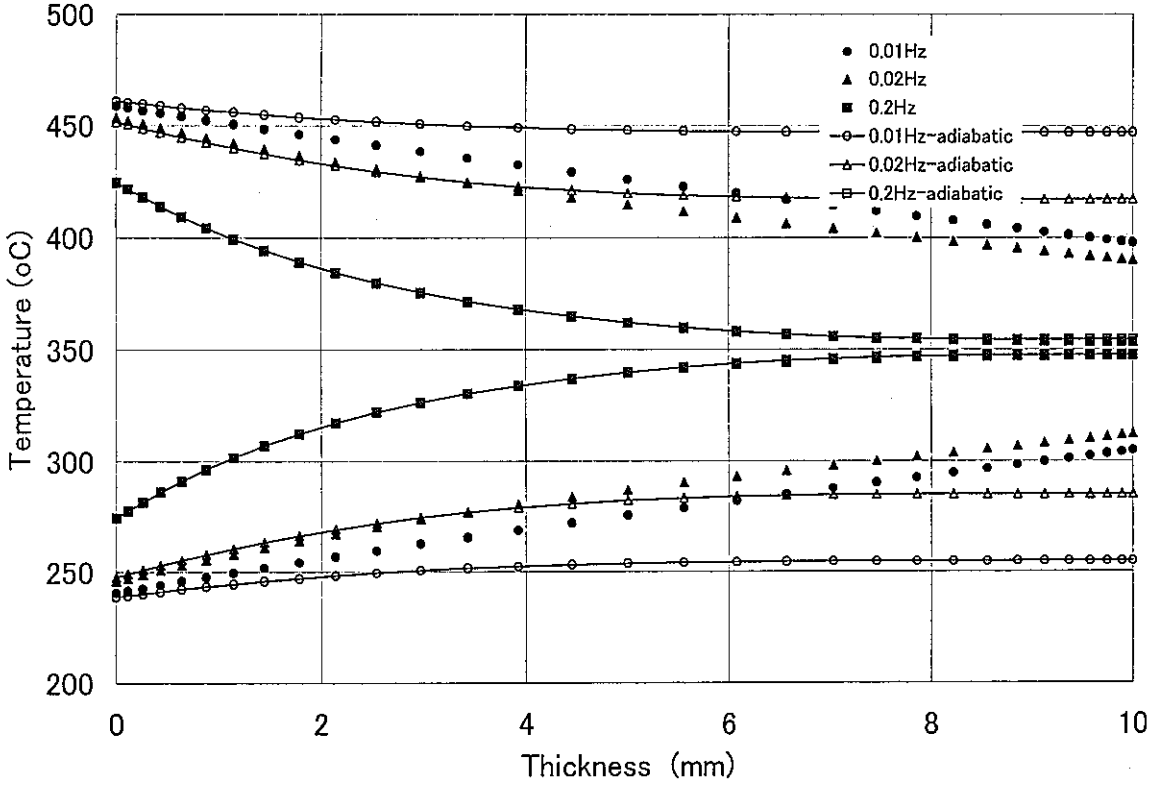

Fig. 2.10 Distribution of the maximum and the minimum temperature at each point during temperature fluctuation

Table 2.8(a) Gain of temperature amplitude obtained by F.E.Calculation (Adiabatic)

f (Hz)	f*	Tiffss-3 (Adiabatic) FEM h=12000kcal/m^2/℃
0.01	0.23	0.93
0.02	0.45	0.85
0.20	4.53	0.63

Table 2.8(b) Gain of temperature amplitude obtained by F.E.Calculation (In sodium)

f (Hz)	f*	Tiffss-3 (In sodium) FEM h=12000kcal/m^2/℃
0.01	0.23	0.91
0.02	0.45	0.86
0.20	4.53	0.63

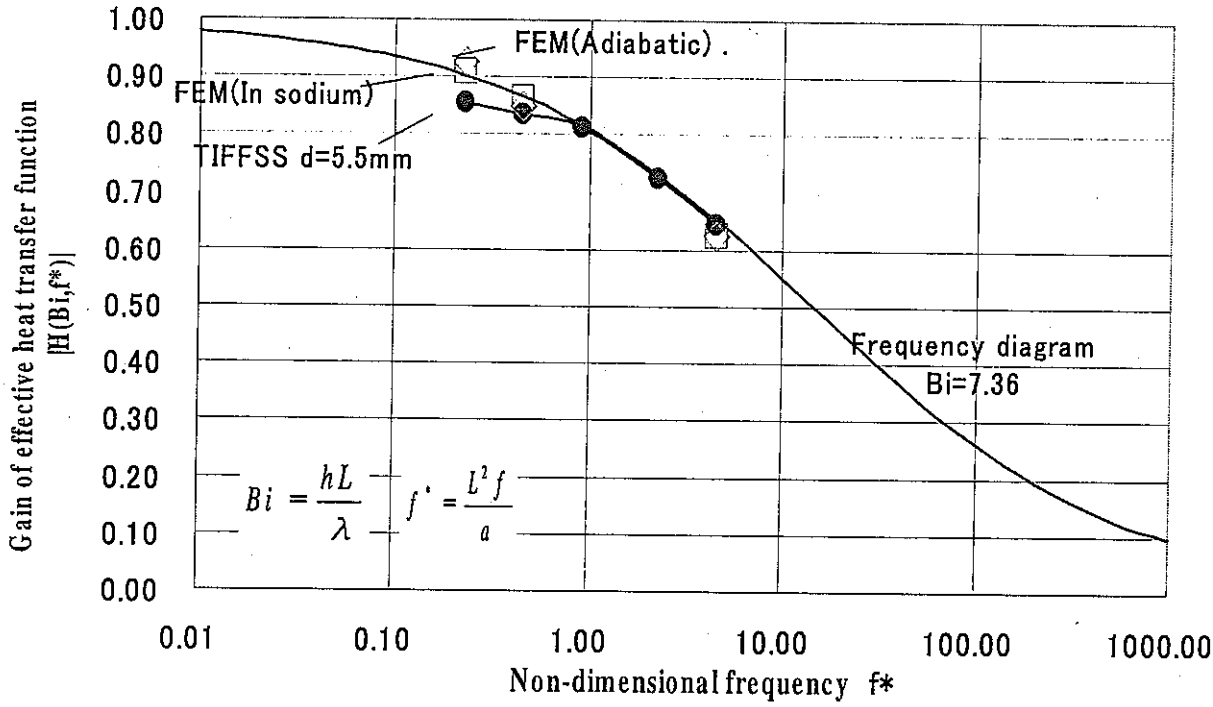

Fig. 2.11 Sensitivity of gain of temperature amplitude to thermal boundary on the back surface

(2) Difference between experimental signal and sinusoidal approximation

The frequency response function method assumes temperature fluctuations of fluid as sinusoidal signal, however actual one of FAENA and TIFFSS experiments were different. For example, a signal of TIFFSS-3 0.02Hz experiment and a sinusoidal approximation were compared in Fig.2.12. To investigate difference of induced thermal stress, temperature response to both an experimental signal of TIFFSS-3 0.02Hz condition and a sinusoidal approximation were calculated by Finite Element Method. The F.E. model was the same as the adiabatic model in Fig.2.7 and Fig.2.8.

Fig.2.13 compares thermal stress responses to an actual fluid temperature and its sinusoidal approximation. Temperature range induced by the experimental signal is larger than one of sinusoidal approximation. The reason is considered that experimental signal has longer holding time at the maximum and the minimum temperature than sinusoidal one. Sensitivity of gains to signal shape shown in Table 2.9 and Fig.2.14 indicates that it can not be negligible.

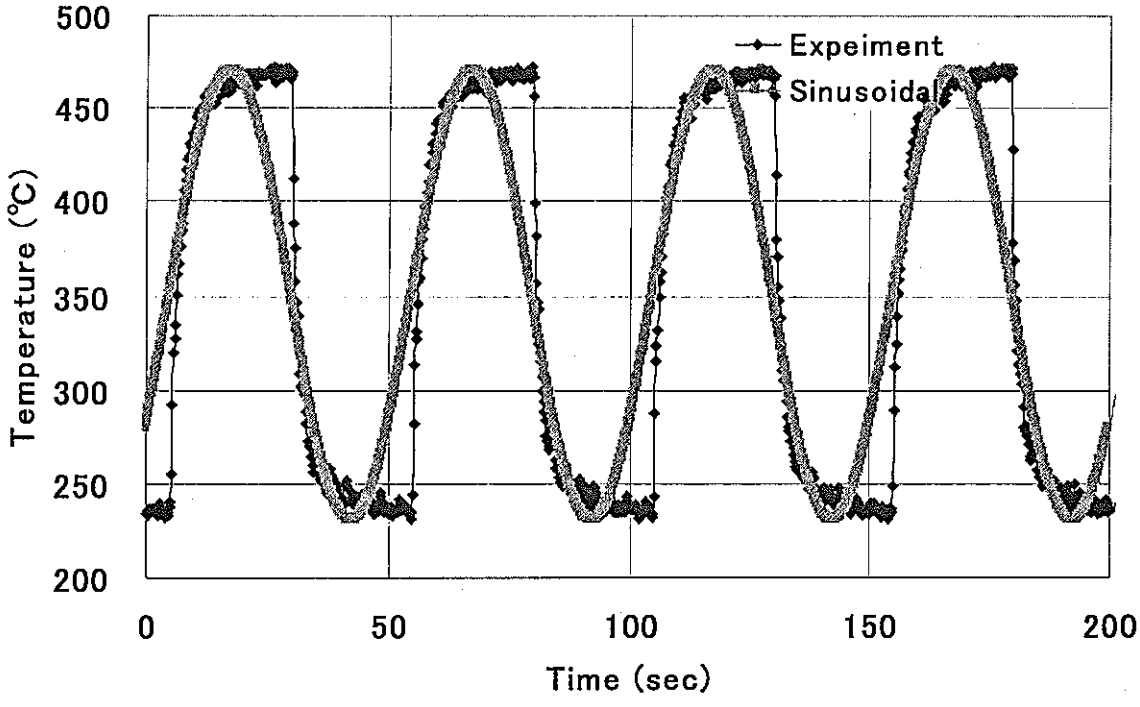

Fig. 2.12 Sinusoidal approximation of fluid temperature fluctuation (0.02Hz)

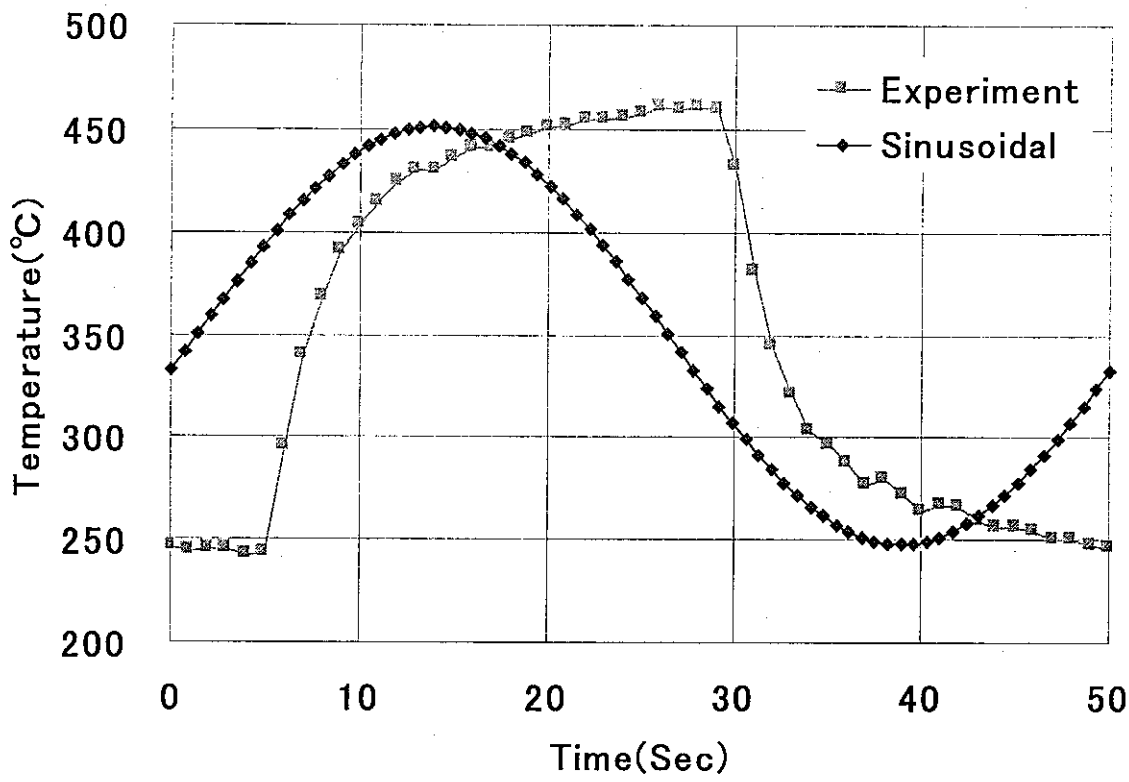

Fig. 2.13 Temperature response to experimental and sinusoidal temperature fluctuations

Table 2.9 F.E. calculated gains of temperature amplitudes under experimental and sinusoidal signals

fluctuation	f (Hz)	f*	Tiffss-3 (Adiabatic) FEM h=12000kcal/m^{2}h℃
Experiment	0.02	0.45	0.90
Sinusoidal	0.02	0.45	0.85

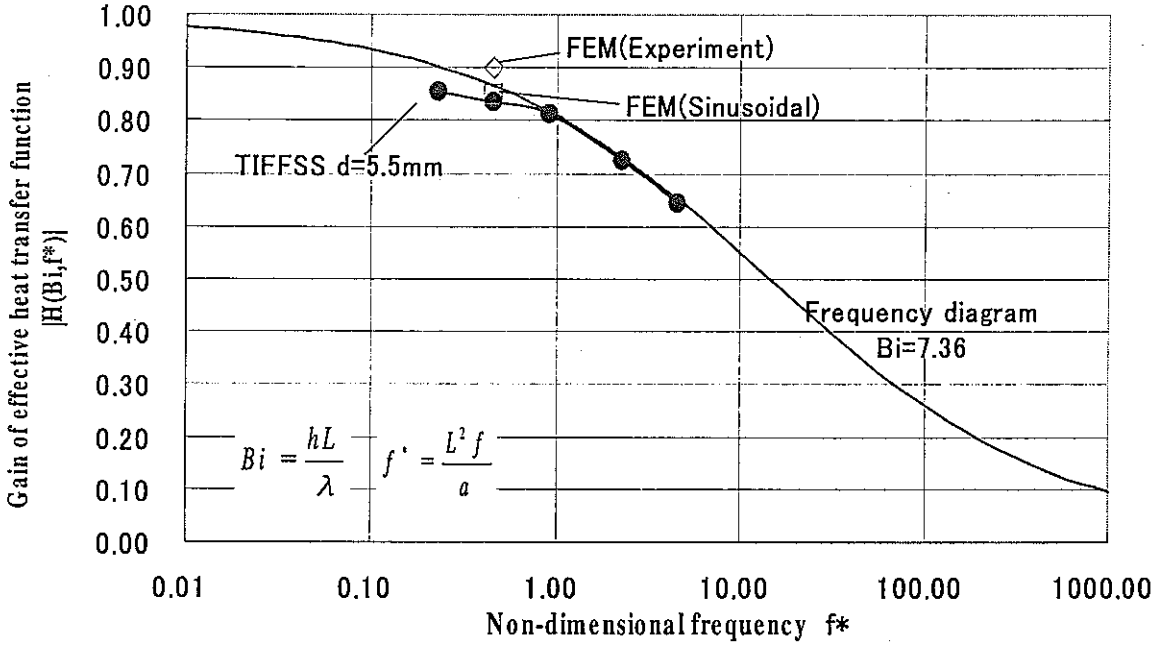

Fig. 2.14 Sensitivity of gain of temperature amplitude to signal shape

(3) Temperature dependency of material properties

Material properties of structures usually depend on temperature. Contrary, the frequency response method assumes constant properties of average temperature. To study influence of temperature dependency, Finite element method calculated both cases of temperature dependent and constant properties.

Obtained temperature responses of the structural surface were compared and results are described in Fig.2.15. Difference of the temperature amplitudes between both material properties was less than 0.5 ℃ and gains of temperature amplitude were approximately the same as in Table 2.10. From these results, temperature dependency of thermal material properties can be negligible.

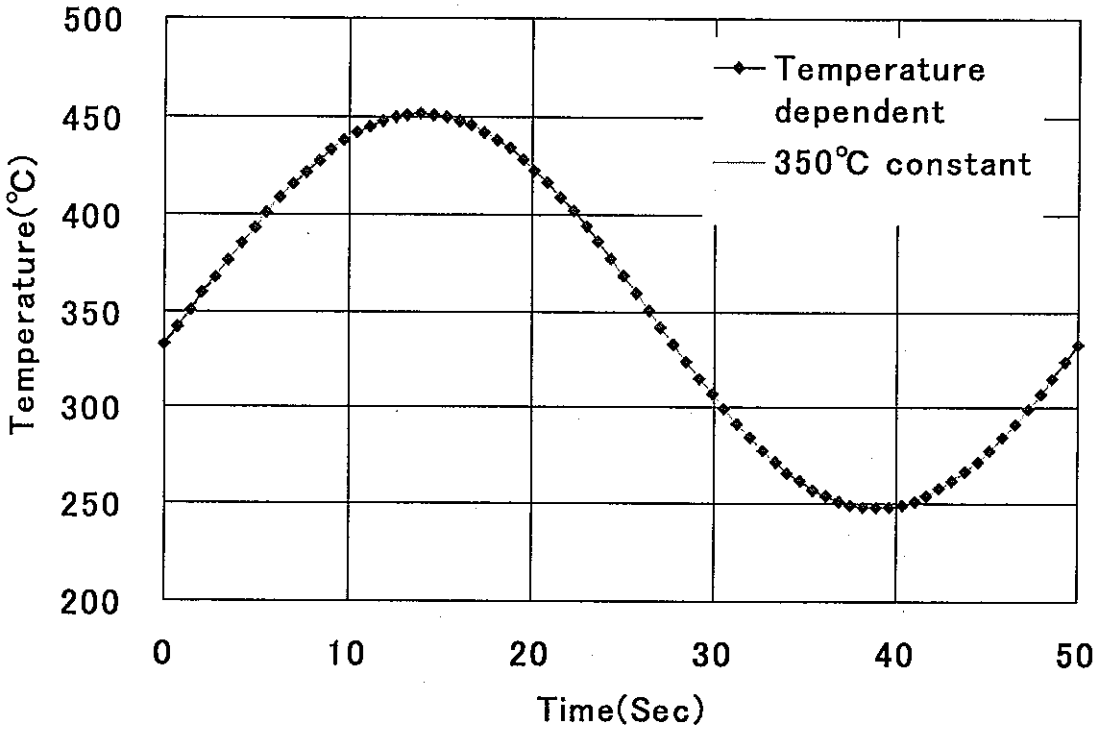

Fig. 2.15 Temperature response of experimental and sinusoidal temperature fluctuations

Table 2.10 F.E. calculated gains of temperature amplitudes under experimental and sinusoidal signals

Material	f (Hz)	f*	Tiffss-3 (Adiabatic) FEM h=12000kcal/m^{2}h℃
Temperature dependent	0.02	0.45	0.85
350℃ constant	0.02	0.45	0.85

3. CEA EVALUATION

3.1. SIMPLIFIED METHODS

As was made by JNC, CEA developed a method for calculating temperature and stress in a wall surrounded by a fluid with a fluctuating temperature. The basic temperature signal is a sinusoidal wave, so that the approach can be applied to random signal by means of Fast Fourier Transform of the original signal. The method is based on analytical results for the one-dimensional problem of the plate submitted to a temperature fluctuating at the surface, the backface being insulated (heat flux equal to zero) :

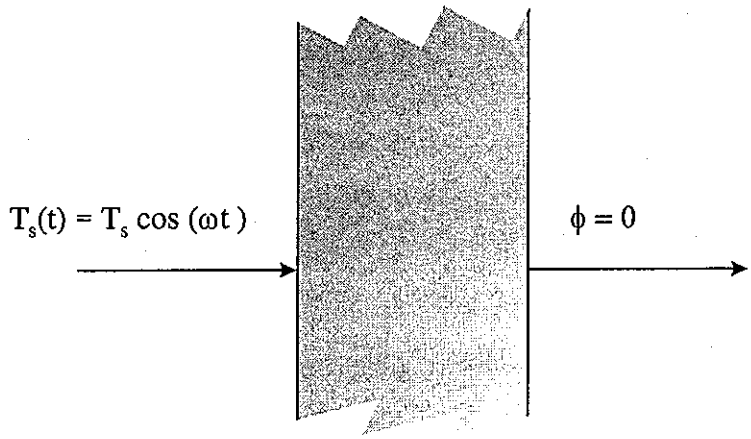

Fig. 3.1 Description of the problem

We can write the temperature in any point at any time as follows [7] (it seems that this problem was first solved by Groeber in 1921 [8]) :

$$\mu = \left[\frac{\omega}{2a}\right]^{1/2}$$
$$P = \cosh[\mu(L-x)]\cos[\mu(L-x)]$$
$$P' = \sinh[\mu(L-x)]\sin[\mu(L-x)]$$
$$Q = \cosh[\mu L]\cos[\mu L]$$
$$Q' = \sinh[\mu L]\sin[\mu L] \qquad (3.1)$$
$$R = \left[\frac{P^2 + P'^2}{Q^2 + Q'^2}\right]^{1/2}$$
$$\psi = Atn\left[\frac{P'Q - PQ'}{P\,Q + P'Q'}\right]$$
$$T(x,t) = T_s\, R\cos(\omega t + \psi)$$

Then, the temperature gradient is numerically estimated inside plate permitting to determine a fictive fluid temperature for various heat exchange coefficients, by means of heat flux continuity at the surface :

$$-h(T_f - T_s) = \lambda\, dT/dx \qquad (3.2)$$

The fluid temperature is equal to $T_f = T_s - \lambda/h\ dT/dx$. Different fluid temperatures can be obtained during the cycle as we assume in a first step that surface temperature is known, λ is known, dT/dx is determined numerically with dx = L/1000 ; h coefficient is considered as a parameter in that case. The problem being linear, that means fluid temperature is proportional to surface temperature in that case, due to the heat flux equation and to the temperature profile inside the plate :

$$dT/dx = T_s\,[\, dR/dx \cos(\omega t+\psi) - R\omega \sin(\omega t+\psi)\,] \qquad (3.3)$$

Then :

$$T_f = T_s\,(\,1 - \lambda/h\,[\, dR/dx \cos(\omega t+\psi) - R\omega \sin(\omega t+\psi)\,]\,) \qquad (3.4)$$

Thus, we not only know phase and attenuation temperatures through the wall, but also fluid to structure heat transfer attenuation and phase delay (the latter is determined numerically by calculating the time delay between fluid and surface temperature maxima). Fluid to structure heat transfer attenuation is defined by Tsmax / Tfmax ratio, Tsmax being maximum of surface temperature and Tfmax the maximum of fluid temperature.

We would like to point out that the same method has been applied to through wall linear temperature gradient, surface peak temperature, mean temperature, so it's now possible to recombine these components to compute surface stress from any signal. (this part will be described in a further report).

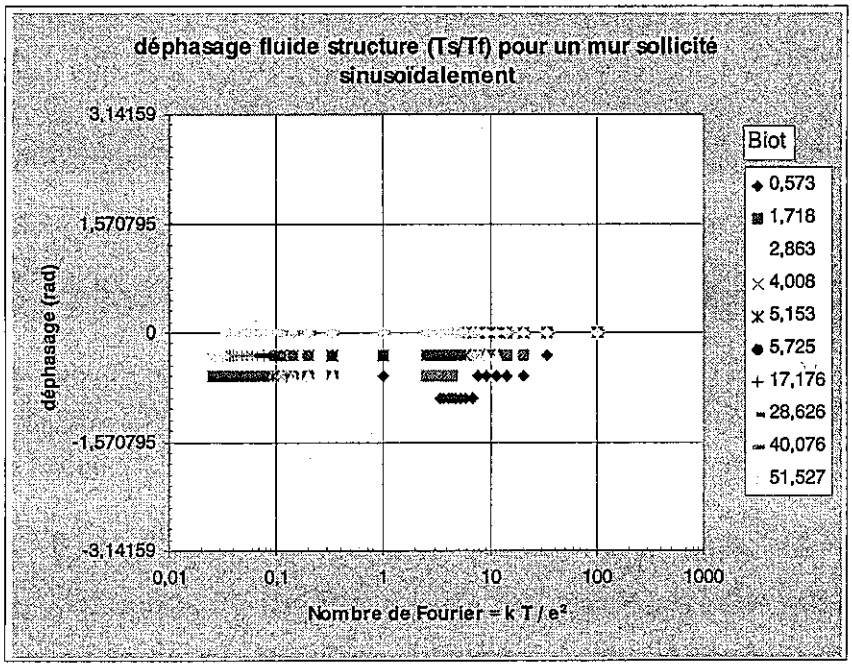

Fig 3.2 Phase delay from fluid to structure during heat transfer

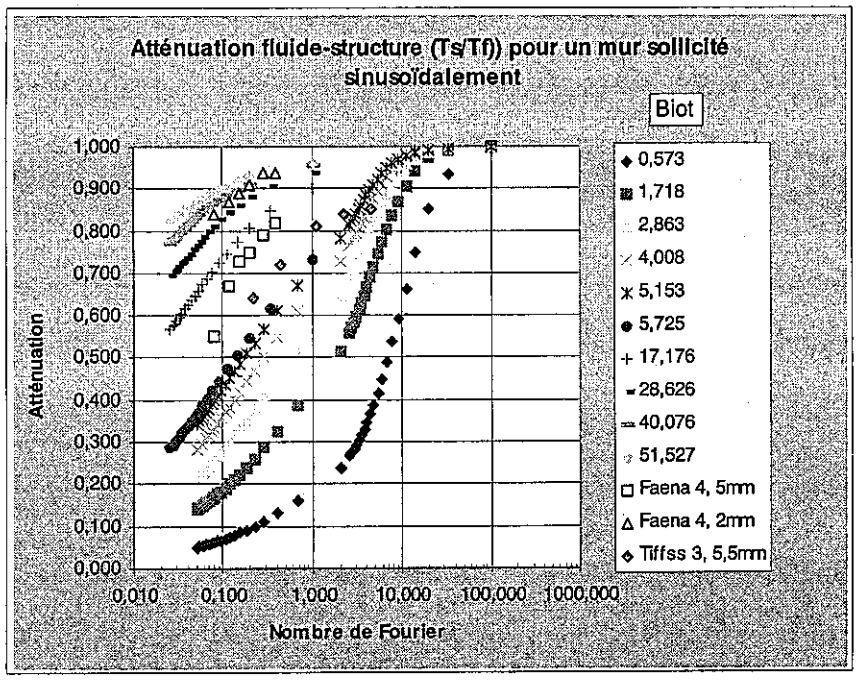

Fig 3.3 Attenuation from fluid to structure during heat transfer

Figures 3.2 and 3.3 show the results of numerical simulations with different frequencies (giving varying Fourier numbers) and the different h coefficient (which gives a set of Biot number), the others parameters being constants (thickness, diffusivity, conductivity). The steps on phase delay diagram are due to the time discretization (20 points were considered as sufficient to define the cycle : these points are chosen to optimize the surface temperature so that sometimes the fluid temperature is not exactly caught. But in practice the error on the maximum is not very large for a sinusoidal signal). Results of FAENA 4th and TIFFSS 3 experiments are placed on the attenuation diagram. As Biot number is equal to 14.1 (details are given thereafter) for FAENA, there is a good agreement between experiments and calculations (for thermocouples in the fluid at 5 mm from the surface) . The case of TIFFSS 3 experiment is more difficult since it is not easy to define a heat transfer coefficient. It can be seen that experimental points are consistent with a Biot number near 5 (for thermocouples in the fluid at 5.5 mm from the surface). If we select Biot number equal to 8.2 for thermocouples at distance 5.5 mm (from JNC evaluation), again we have a good agreement between experiment and calculation as shown in tables below :

Table 3.1 Comparison of predicted attenuation ratios with measurements

f (Hz)	Fourier number	Biot number	FAENA-4th (L=15mm,d=5mm) Measured gains	FAENA-4th (L=15mm,d=5mm) CEA Predicted gains
0.05	0.391	14.1	0.82	0.79
0.07	0.279	14.1	0.79	0.77
0.10	0.196	14.1	0.75	0.73
0.13	0.150	14.1	0.73	0.71
0.17	0.115	14.1	0.67	0.68
0.25	0.078	14.1	0.55	0.64

f (Hz)	Fourier number	Biot number	Tiffss-3 (L=10mm,d=5.5mm) Measured gains	Tiffss-3 (L=10mm,d=5.5mm) CEA Predicted gains
0.01	4.40	8.19	0.85	0.92
0.02	2.20	8.19	0.84	0.84
0.04	1.10	8.19	0.81	0.77
0.10	0.440	8.19	0.72	0.68
0.20	0.220	8.19	0.64	0.61

These tables correspond to the following diagram :

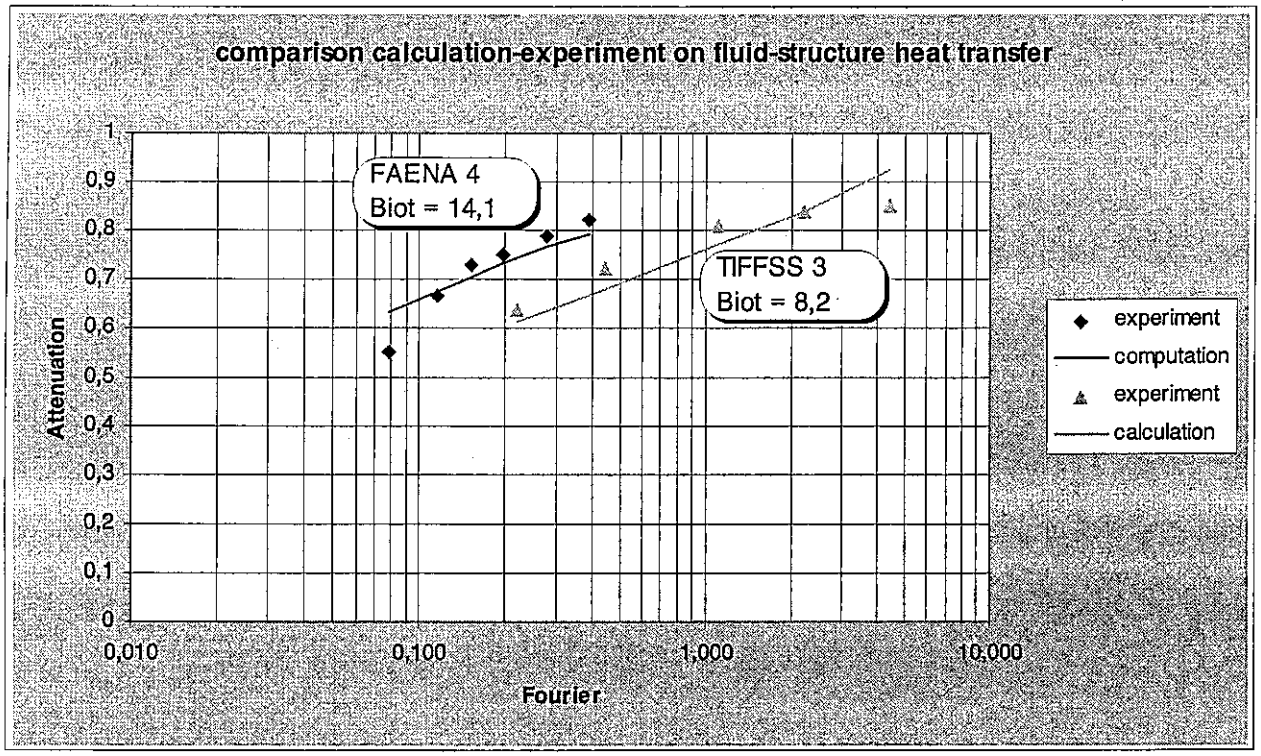

Fig 3.4 Precise comparison between calculated and measured attenuation during heat transfer

To estimate Biot number, the main difficulty is to determine heat exchange coefficient : this can be done through Skupinski analysis [3]. Skupinski equation represents a correlation between Peclet number and Nusselt number, established by interpretation of thermal measurements during liquid metal flow experiments. With a flow velocity of 0.5 m/s and an internal diameter of 24.9 mm, we obtain a Reynolds number about 35000 at 350°C. As Prandtl number is near 0.0054 at this temperature, Peclet number is equal to 189 ; application of Skupinski gives a Nusselt of 6.23. It is observed that Peclet number is not highly temperature dependent, because Reynolds number increase is compensated by Prandtl decrease so that Peclet is almost constant with temperature. Considering that thermal conductivity is about 19.6 J/s/m/°C, we finally obtain h = 18500 W/m2/°C, corresponding to a Biot number of 14.1 .

3.2. FINITE ELEMENT CALCULATIONS

These calculations were made with CASTEM 2000 code in order to verify temperatures given by simplified methods. With the mesh of the figure 3.5 precisely representing the assembly of the plate and his support in 2D, we impose in the internal channel the experimental temperatures of sodium during a cycle, and at the level of the instrumented section z = 43, with a coefficient h = 18000 W/m /°C. According to the experimental conditions of flow, this coefficient is nearly the same as indicated in the previous section. At outside, the exchange coefficient is much lower since the specimen is in contact with Argon. The duration of the cycle is 8.2s and the temperature variation is 272°C. Initially, it is supposed that the specimen is at the average temperature of the tests (for an easier stabilization of the thermal cycles), only one cycle is sufficient to reach the stationary cycle. It can be seen on the figure 3.6 that the level of the variations of the temperatures measured on the internal surface is well reproduced.

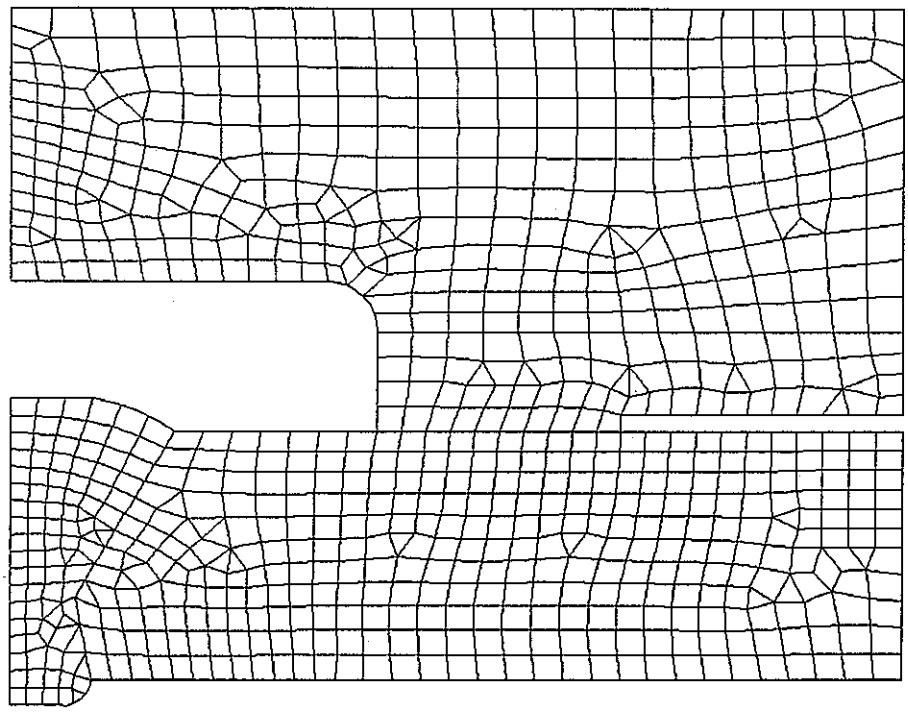

Fig. 3.5 Mesh used for the finite element calculations of Faena 4 (f ~ 0.125 Hz)

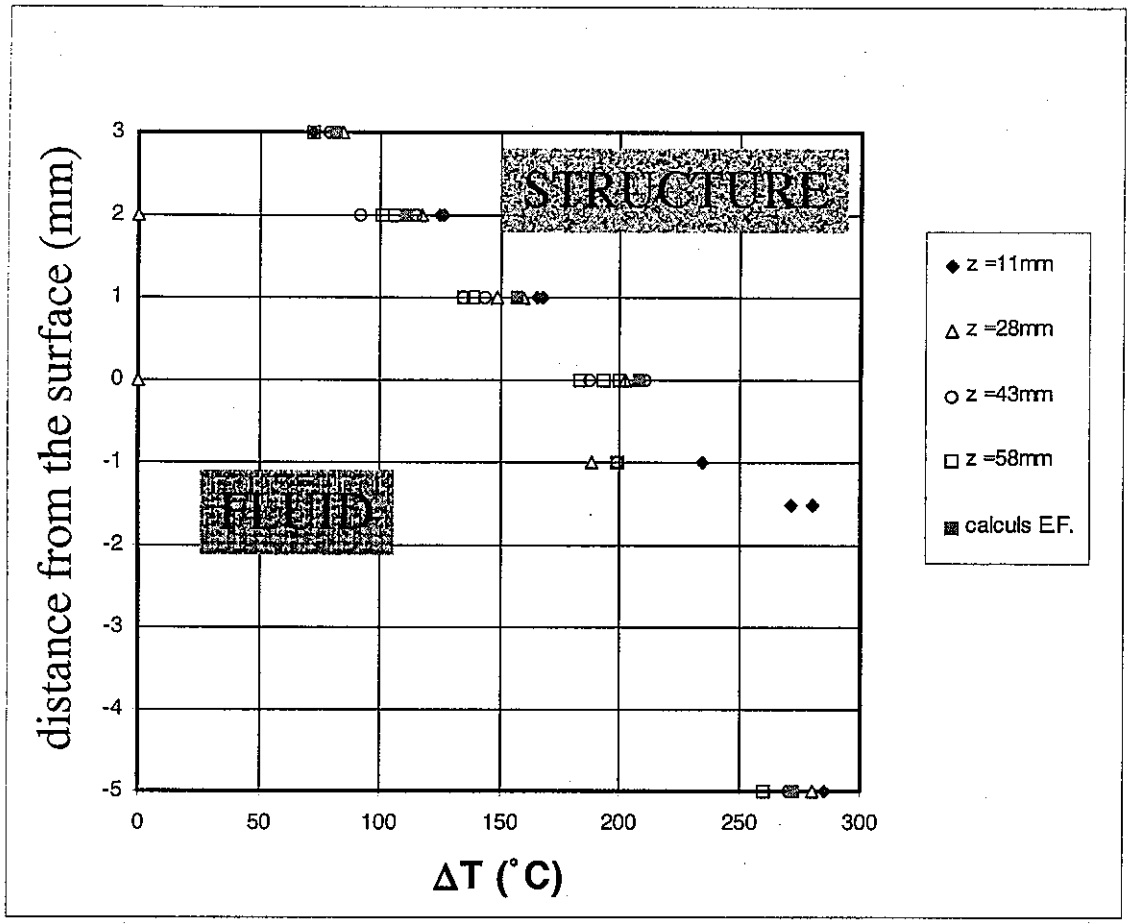

Fig. 3.6 Comparison between measured (in all sections) and calculated (in section z=43 mm) temperatures

4. DISCUSSIONS

4.1. INTERCOMPARISON

CEA and JNC have adopted similar approaches for evaluation of temperature. Both approaches are based on frequency response analysis to sinusoidal temperature fluctuations. The unique difference is the calculation method of heat transfer from fluid to structural surface even though basic theory is the same.

Gains of temperature range between fluid and structural surface were compared among measurements, CEA predictions, and JNC ones as shown in the next tables. Here, gains from fluid at sufficient distances from the structural wall were selected, since there remains many discussions to evaluate fluid near the boundary layer. All results are within a small scatter band. Main reason of difference is Biot number i.e. heat transfer coefficient.

Table 4.1 Intercomparison of measured gains with CEA and JNC predictions

f (Hz)	FAENA-4th (L=15mm,d=5mm) Measured gains	FAENA-4th (L=15mm,d=5mm) CEA Predicted gains	FAENA-4th (L=15mm,d=5mm) JNC Predicted gains
0.05	0.82	0.79	0.87
0.07	0.79	0.77	0.84
0.10	0.75	0.73	0.82
0.13	0.73	0.71	0.80
0.17	0.67	0.68	0.77
0.25	0.55	0.64	0.73

f (Hz)	Tiffss-3 (L=10mm,d=5.5mm) Measured gains	Tiffss-3 (L=10mm,d=5.5mm) CEA Predicted gains	Tiffss-3 (L=10mm,d=5.5mm) JNC Predicted gains
0.01	0.85	0.92	0.90
0.02	0.84	0.84	0.87
0.04	0.81	0.77	0.82
0.10	0.72	0.68	0.73
0.20	0.64	0.61	0.65

4.2. ADEQUACY OF HEAT TRANSFER MODEL

The frequency response function method was suitable to evaluate temperature attenuation of FAENA 4th and TIFFSS-3 experiments, when appropriate heat transfer coefficients were given. It means that the effective heat transfer function with assumption of constant heat transfer coefficients can approximate thermal phenomena of FAENA 4th and TIFFSS-3 experiments. However, applicable area of heat transfer coefficient equations is limited. From a theoretical point of view, usage of constant heat transfer coefficient is questionable for non-stationary phenomena. Buffet.J.C. and Tenchine,D. have developed the attenuation evaluation method based on the diffusion model[9]. Sensitivities of temperature attenuation to frequencies were calculated by this model and were compared with one of the effective heat transfer function.

In the case of FAENA 4th, attenuation from fluid at 2mm and at 5mm to structural surface were evaluated.

(1) d=2mm

Their method evaluates heat transfer from fluids to structures by conductive layers with a certain thickness y. For evaluation of attenuation from fluid at 2mm, y value was assumed to be 2mm. Considering heat transfer from turbulent convection, this method uses the effective thermal diffusivity α' that can be evaluated from the thermal diffusivity of fluid by the next way.

The thermal diffusivity of sodium at 400℃ is

α = 6.59872E-05 m^2/sec. (4.1)

Friction velocity

$$u^* = \sqrt{\frac{\tau}{\rho}} \tag{4.2}$$

was calculated from average velocity u= 0.413m/s as

u*=0.313m/s, (4.3)

under assumption of 1/7 power law

$$\frac{u}{u^*} = 8.74\left(\frac{u^* y}{\rho}\right)^{\frac{1}{7}}, \text{ Re} < 100{,}000 . \tag{4.4}$$

for velocity field. Here, Reynold's number of FAENA is 21300.

When assuming logarithmic law

$$\frac{u}{u^*} = 5.75\log\left(\frac{u^* y}{\nu}\right) + 5.5 \tag{4.5}$$

for velocity field, Friction velocity becomes

u*=0.0234m/s. (4.6)

From above values, the turbulent Peclet number is

$$Pe_* = \frac{u^* y}{\alpha} = \begin{cases} 10.6 \ (1/7 \ Power \ law) \\ 0.709 \ (Logarithmic \ law) \end{cases}. \tag{4.7}$$

This value from 1/7 Power law is slightly out of validated range[11].

From above values, the effective diffusivity is

$$\alpha' = \alpha \ \mu \ Pe_* + \alpha = \begin{cases} 4.16\times10^{-4} m^2/\sec \ (1/7 \ Power \ law) \\ 8.94\times10^{-5} m^2/\sec \ (Logarithmic \ \text{law}) \end{cases} \quad \mu = 0.5. \tag{4.8}$$

A 2mm thickness conduction model with the normal diffusion (Eq.(4.1)) and the effective diffusivity (Eq.(4.8)) predicted gains of temperature range. The results were compared with experimental ones and prediction by the effective heat transfer function as the next figure.

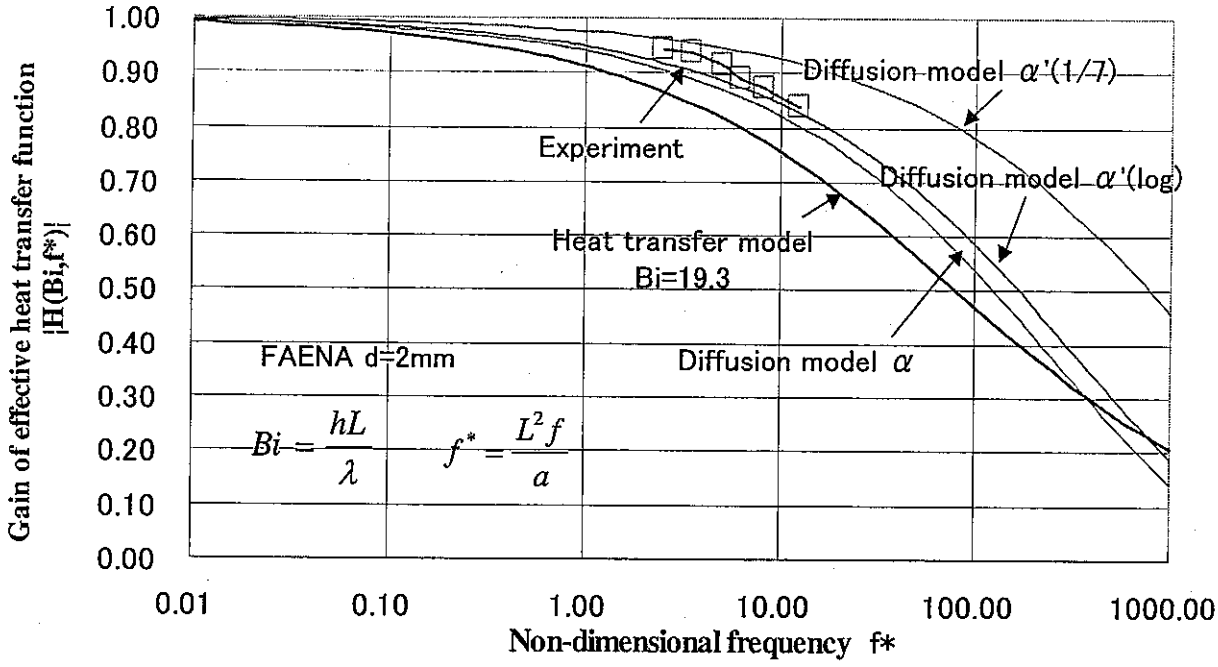

Fig.4.1 Comparison of gains among experiments, a heat transfer model and diffusion models (FAENA d=2mm)

Fig. 4.1 explains that the diffusion model with the effective thermal diffusion from Logarithmic law has good agreement with measurements. Both experiments and predictions by the diffusion model show that the heat transfer model is a little bit conservative.

(2) d=5mm

Friction velocities at 5mm from the wall were calculated from average velocity u= 0.413m/s as

$$u^* = \begin{cases} 0.313 \ (1/7 \ Power \ law) \\ 0.0209 \ (Logarithmic \ law) \end{cases}. \tag{4.9}$$

With the thermal diffusivity of sodium at 400℃, distance y=5mm from the wall and friction velocities, the turbulent Peclet number Pe* is

$$Pe_* = \frac{u^* y}{\alpha} = \begin{cases} 23.7 \ (1/7 \ Power \ law) \\ 1.58 \ (Logarithmic \ law) \end{cases}. \tag{4.10}$$

This value from 1/7 Power law is out of validated range[9].

From above values, the effective thermal diffusivity α' is

$$\alpha' = \alpha\ \mu\ Pe_* + \alpha = \begin{cases} 8.47\times10^{-4}\,m^2/\sec\ (1/7\ Power\ law) \\ 1.18\times10^{-4}\,m^2/\sec\ (Logarithmic\ \text{law}) \end{cases} \quad \mu = 0.5. \qquad (4.11)$$

A 5mm thickness conduction model with the normal diffusion (Eq.(4.1)) and the effective diffusivity (Eq.(4.11)) predicted gains of temperature range. The results were compared with experimental ones and prediction by the effective heat transfer function as the next figure.

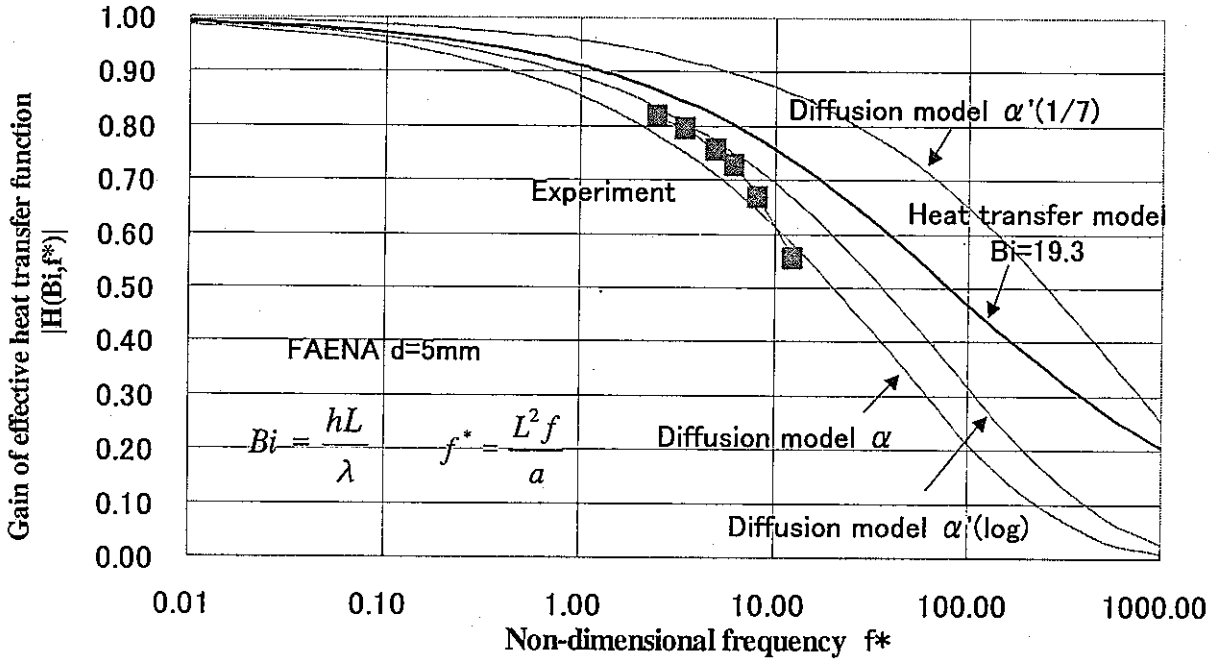

Fig.4.2 Comparison of gains among experiments, a heat transfer model and diffusion models (FAENA d=5mm)

Fig. 4.2 explains that the diffusion model with the effective thermal diffusion from Logarithmic law has good agreement with measurements, and has a weaker sensitivity to frequency than the heat transfer model. Advantage of the diffusion model is its applicability to fluids near the wall. So that frequency response function based on the diffusion model is planned in the next phase.

4.3. OTHER DISCUSSIONS

Another point for further investigations concerns the time length of temperature signals : it is not always possible to obtain long duration signal measurement or calculation ; some works are needed for extrapolation of temperature fluctuations to long duration. It is not an easy task since temperature fluctuation is always limited in range and classical statistics should not be applied ; another reason is that sample of data must be stabilized which condition is not always practically reached.

Furthermore, errors of the frequency response function from sinusoidal approximation of temperature fluctuation can not be negligible. One of ideas to improve this method is application of Fourier decomposition method, which will be studied, in the following reports. There is possibility that electric control system can realize sinusoidal temperature fluctuations in sodium experiments. JNC is planning to introduce an electric control system to TTS facility.

ACKNOWLEDGEMENT

The authors are deeply indebted to Dr. D. Tenchine of CEA-Grenoble for his suggestion to evaluation of heat transfer coefficients. Several helpful discussions in thermal hydraulic field with Dr. T.Muramatsu, Mr. H.Kamide, and Mr. M.Nishimura of OEC/JNC, Dr. P.Roubin of CEA-Cadarache, and Dr. J.P.Simoneau of Framatome are gratefully acknowledged. It is very thankful in coordination of cooperative study between CEA and JNC by Dr. J.C. Astegiano, Dr. C.Poette and Dr. M.T. Cabrillat of CEA-Cadarache and Dr.M.Morishita of OEC/JNC.

REFERENCES

[1] Kasahara,N. and Lejeail, Y., Benchmark problems on thermal striping evaluation of FAENA and TIFFSS sodium experiments, JNC TN9400 2001-006,(2000)

[2] Kasahara,N., Frequency response function method for evaluation of thermal striping phenomena , JNC TN9400 2001-005,(2000)

[3] Skupinski, E, Mixed Convection of the Shell of a Horizontal Na-to-NaK Heat Exchanger, "Progress in Heat and Mass Transfer. Vol. 7. Heat Transfer in Liquid Metals", Pergamon Press Ltd., Oxford, England, 527-537, (1973)

[4] Subbotin, et al., Atomnaya Energiya,13-10, 380 (1962)

[5] Gardon, R. and Akfirat, J.,C., Int.J. Heat Tranfser 8 (1965), Trans. ASME Ser.C. 88-1 1261, (1965)

[6] Iwata,K., FINAS Version 13.0 User's manual, PNC TN9520 95-014, (1995)

[7] Max. Jakob, Heat transfer , John Wiley and Sons, Inc., 4th edition of (1955)

[8] Groeber H. , Die Grundgesetze der Waermeleitung und des Waermeueberganges , Julius Springer, Berlin, (1921)

[9] Buffet.J.C. and Tenchine,D., Transfer of temperature fluctuations across boundary layers in turbulent liquid metal flows, ASME,PVP Vol.98 pp153/157(1985)